AN AIRBEARING-BASED TESTBED FOR MOMENTUM-CONTROL SYSTEMS AND SPACECRAFT LINE OF SIGHT

Mason A. Peck[†] and Andrew R. Cavender[‡]

Honeywell has developed a spacecraft attitude-dynamics testbed that is designed to assist in research, demonstration, and validation of hardware and software architectures for such spacecraft. The testbed offers high-agility slew and scan capability (via six 225 ft-lb CMGs) with structural control (via active vibration-isolation and payload-steering platforms and discrete high-performance structural dampers). The combination of an interferometry-based line-of-sight metrology system capable of 15 nanoradians resolution and a large range-of-motion spherical airbearing offers a unique environment for realtime, hardware-in-the-loop testing of innovative controls and dynamics concepts in spacecraft design. This paper describes the facility's capabilities, including its ability for autocoding MATLAB/Simulink models, attitude-control and estimation design, structural design, and disturbance-mitigation measures. It also presents recent data showing the pointing performance of a structure driven by a momentum control system.

INTRODUCTION

One of the fundamental principles that govern spacecraft design is that the system must work the first time. Any options for reconfigurability are generally designed in because, once a space system has been launched, the cost of launch and operations associated with on-orbit repair are usually seen as prohibitively high. This principle motivates the rigorous analysis and testing that spacecraft undergo. Detailed simulations and realistic ground tests of the launch and on-orbit environments are routine in the development of modern spacecraft, and the deployment of sophisticated systems is often constrained by what can be proven successful by simulation or test before launch.

Realistic testing of attitude dynamics and control for flight hardware is rarely undertaken because reproducing vacuum and microgravity conditions poses unique challenges in a terrestrial environment. Some satellites, generally only those whose flexible dynamics can be treated as negligible, have in fact been tested this way, with the help of air bearing simulators[1]. But as the objectives for earth- and space-observing satellites become more extreme, requiring ever finer pointing for longer durations, the effects of structural flexibility become more important.

[†] Principal Fellow, Special Projects, Honeywell Space Systems, Glendale, Arizona. Member AAS.
[‡] Staff Engineer, Special Projects, Honeywell Space Systems, Glendale, Arizona.

While the structural dynamics of spacecraft receive detailed attention, the propagation of jitter throughout the structure is rarely based on accurate models of the structural dynamics. One reason is that structural-dynamics models often capture no more than the first few modes accurately; higher-frequency modes, which can be at least as important for jitter, are difficult to pin down. Conservative estimates usually result when these analytical shortcomings are acknowledged. Large-angle attitude maneuvers, particularly under the actuation of control-moment gyros (CMGs) further complicate this picture. Honeywell and others have recognized the need for testing spacecraft hardware in a realistic environment to better understand the complex interactions of actuator dynamics with structural response.

This need motivates our development of the Momentum Control System and Line of Sight (MCS/LOS) Testbed. Two views of its current configuration are shown in Figure 1. The facility is intended to provide a unique environment for testing innovative

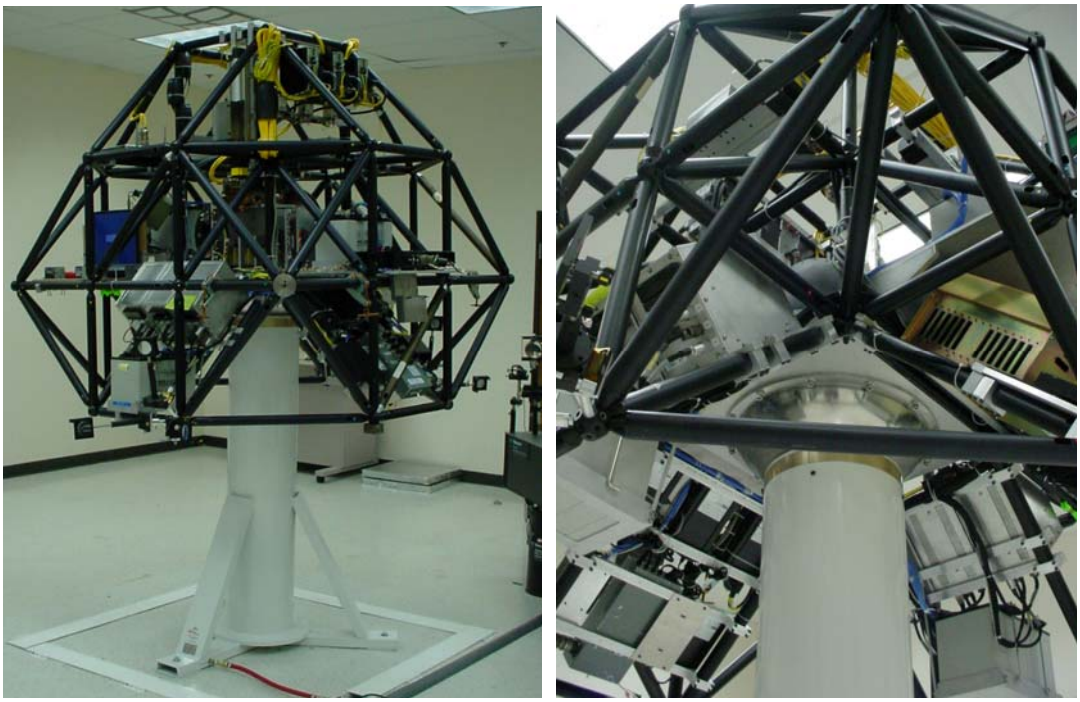

Figure 1. Two Views of the 2003 MCS/LOS Testbed during Maneuvers

controls and dynamics concepts in spacecraft design. Its objectives include the study and evaluation of momentum-control systems (such as arrays of CMGs) in the presence of representative structural dynamics and large-angle attitude motion. This paper provides an overview of the testbed's development in 2003, including an assessment of its current performance and our plans for enhancing the setup in 2004. We discuss the design of the testbed, its hardware, and its software.

SYSTEM DESIGN

Objectives

The MCS/LOS Testbed is meant to provide a platform for fundamental research in momentum control and line of sight for agile, precision-pointed spacecraft. It also offers Honeywell, its partners, and its customers opportunities for developing and validating flight hardware and software. These intended uses require the testbed to offer high-agility slew and scan capability with integrated structural control. They also demand a line-of-sight metrology system capable of sub-microradian resolution and a large range-of-motion spherical airbearing.

MCS Concept

Before discussing the details of the testbed design, we present Honeywell's concept of a momentum control system (MCS). An MCS embodies the benefits inherent in procuring a fully integrated momentum control system as opposed to the historical approach of procuring individual actuators (control moment gyroscopes, momentum wheels, or reaction wheels), isolators, and/or structures, and incurring the cost and schedule of the customized integration of these components.

The potential benefits of up-front integration of some, or all, of the ACS system has been recognized by the spacecraft community for some time. Unfortunately, the customized process of matching ACS components to satisfy mission requirements has not led to a consistent architecture across the entire spectrum of ACS components. In the case of mature technologies such as momentum-control devices, and as the demands on spacecraft designers time increases, it makes more sense to integrate this important ACS component into a single assembly

A momentum control system is an optimally integrated system that develops output torque in a desired direction. It contains actuator(s) for managing spacecraft momentum and torque needs for attitude control; command and control electronics to accurately control and report the system state; embedded software for processing external commands, implementation of control/steering laws, and implementation of internal housekeeping and fault management functions; and an integral structure that incorporates some form of vibration-isolation capability. It offers a simple, deterministic interface for hardware integration and performance analysis.

The simplified block diagram in Figure 2 shows the basic functionality that resides in the MCS. This architecture reduces the control of the entire momentum control subsystem to a compact, efficient implementation that allows the ACS designer to concentrate development efforts on other, unique elements of spacecraft design.

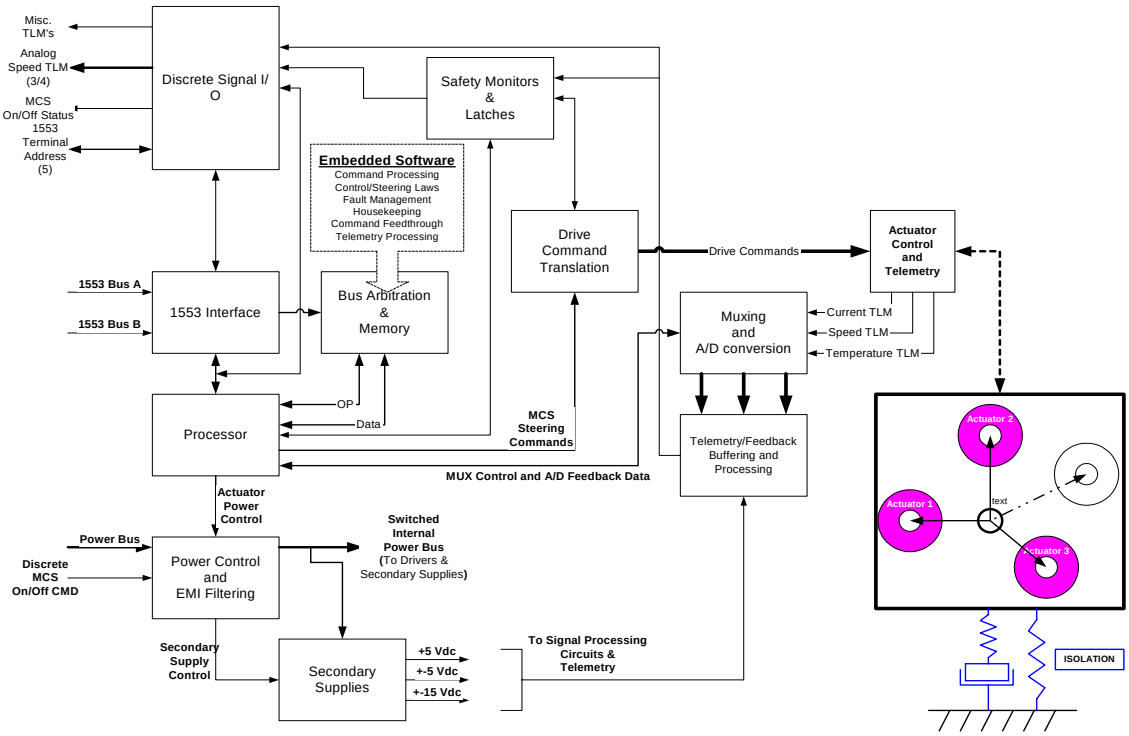

Figure 2. Simplified MCS Block Diagram

We argue that the integrated system performs more efficiently in several ways than a comparable distributed system that does not effectively integrate the functions identified above: weight, power, cost, volume, ease of integration, predictability of integrated performance, and fault response. Figure 3 shows a hardware realization of an integrated MCS that utilizes four momentum actuators. The control electronics, actuators, and vibration-isolation system are all contained within the MCS. Utilizing this approach a spacecraft prime contractor would route a single set of power and signal cables to the unit. Intra-unit cabling then distributes the necessary signals to the MCS subsystems.

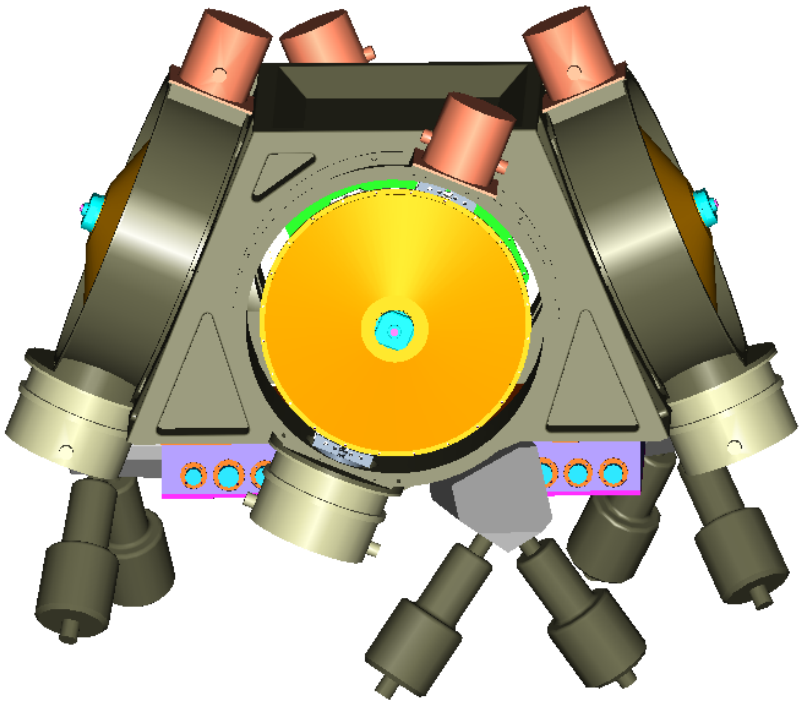

Figure 3. Example of an Integrated MCS Consisting of Four 50 ft-lb-sec CMGs, Embedded Control and Electronics, and Hybrid Active/Passive Vibration Isolation

The MCS/LOS testbed has been and continues to be used to evaluate the performance of such systems in terms of their ability to avoid internal singularities, offer low-jitter performance, and demonstrate autonomous fault responses. Internal and customer-funded projects of this type are planned for 2004.

Structural Control

Vibration isolation integral to an MCS provides a weight-efficient method of attenuating disturbances in six degrees of freedom (DOF). A kinematic mount—a six-strut hexapod or Stewart platform—helps decouple actuator disturbances from local structural behaviors. While this principle applies to individual wheels or CMGs, the integrated MCS approach significantly reduces the amount of hardware and effort needed to accomplish the same goal. For example, an array of 6 CMGs can be isolated as an MCS with only 6 struts, while isolating 6 individually mounted CMGs would require 36. Also, as the spacecraft rotates and applies a so-called base rate on the MCS, constraint torques due to gyroscopic interaction deform the structure; but because of the 6DOF isolation in an MCS, these bending moments are not passed to the spacecraft structure.

The resulting impact on jitter and jitter analysis is substantial: an isolated array can introduce significantly less vibration into the bus structure, which in turn represents lower payload jitter. Conversely, for a given level of jitter performance, an MCS can be

built with lower-precision, hence lower-cost, components whose higher vibration on a per-actuator basis is attenuated by the isolation. Incorporating an MCS therefore offers higher performance per unit cost.

The MCS/LOS Testbed currently includes two forms of structural control. One is distributed damping throughout the testbed, in the form of D-Struts™ that are placed strategically among the truss elements that make up the bus structure. They can be interchanged with rigid struts. This form of structural control can be used to evaluate the impact of explicit damping in the design of isolated bus/payload structures. The other form of structural control is a vibration isolation, suppression, and steering system (VISS), which combines passive isolator technologies with active (voice-coil) control. The hybrid isolator offers linear performance at high frequency due to the passive system and low-frequency attenuation (to eliminate peaking at resonance) due to the active system. The VISS currently in use on the testbed supports an MCS consisting of six tiny CMGs and is the flight spare for a BMDO Space Technology Research Vehicle (STRV) spacecraft, which successfully demonstrated the VISS from 1994-1996[2,3].

Testbed Subsystem Design

The testbed includes all the subsystems that are typically associated with spacecraft: attitude control (ACS), power, thermal, telemetry and command, structure, propulsion, and a payload. All functionality resides onboard the testbed—no tethers connect it to the rest of the lab, limiting environmental disturbances to primarily aerodynamic effects. In addition, the MCS/LOS Testbed lab includes a separate room that serves as a ground station, where operators send commands to task the spacecraft and receive and log realtime telemetry.

The control functionality, including attitude control, payload control, telemetry and command, and certain housekeeping tasks are handled by a dSPACE system that includes a number of A/D and D/A boards, digital I/O channels (including various RS422 protocols), a 1553 interface, and a DS1005 processor. This system, shown in Figure 4, allows MATLAB/Simulink realizations of controls architectures to be autocoded via Realtime Workshop, compiled, and uploaded to run on the testbed in a fairly seamless fashion. It provides what amounts to rapid-prototyping capability for spacecraft controls. Using Simulink also allows the controls architecture to be modular, a feature that allows different attitude-control or MCS-control algorithms to be evaluated without re-validating the entire code. The generic nature of the dSPACE system simplifies integrating bus and payload hardware.

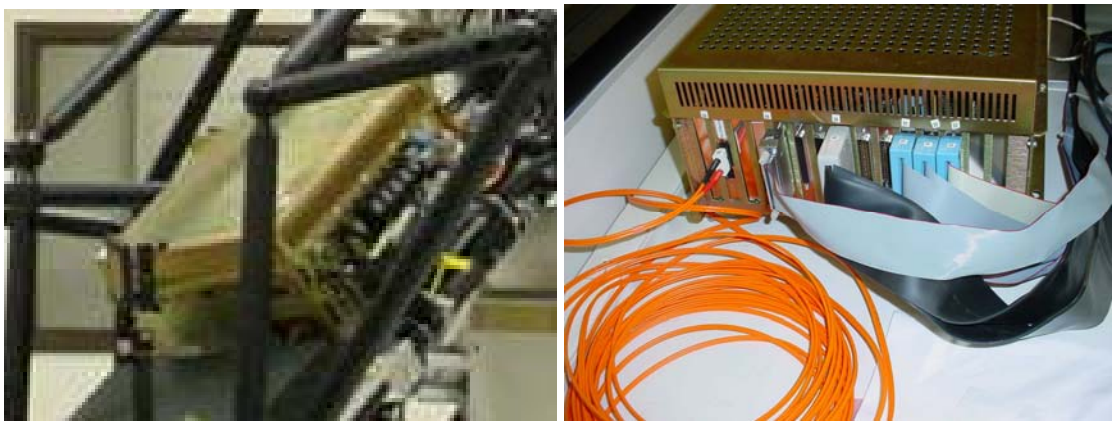

Figure 4. dSPACE System Installed on Testbed (left); dSPACE I/O (right)

Attitude-control hardware includes a Honeywell HG1700AG30 ring-laser gyro capable of better than 1^{o}/hr rate bias and a three-axis accelerometer from which the gravity vector can be estimated as an aid in attitude determination.

Since one of the objectives of the MCS/LOS Testbed is to evaluate MCS designs, the ACS actuators are necessarily interchangeable. The current configuration is one that uses six former aircraft directional gyros that have been rebuilt to function as single-gimbal CMGs. Each stores approximately 0.25 ft-lb-sec of angular momentum and can output about 1 ft-lb of torque. Compared to CMGs built for spaceflight, the gimbal control is low performance: gimbal angles are measured with somewhat noisy potentiometers, and the rate loop is closed at about 5 Hz. These performance parameters are acceptable for individual CMGs because once they are integrated into an MCS and their disturbances attenuated through structural control, the system performance is much better. Table 1 summarizes some of the performance parameters for these tiny CMGs.

Table 1. Performance Parameters for Testbed CMGs

Performance Parameter	Value
Total Mass per CMG (w/o control electronics)	3 lb
Angular Momentum	0.25 ft-lb-sec
Output Torque	1.0 ft-lb
Max. Base Rate at Max Output Torque	4 rad/sec
Rotor Speed	22,000 RPM
Rotor Inertia	0.00011 sl-ft^2
Gimbal Rate Loop Crossover Frequency/GM	5 Hz/20 dB

The CMGs are modified DG-312 Directional Gyros, built by Sperry in the early 1970s. The two synchros were removed and replaced with a torque motor and potentiometer; a tachometer was added to read rotor speed; and four holes were added to

the casing for depth gage access to a precision surface on the rotor's frame. Figure 5 is a schematic of the gimbal and the rotor. The gimbal axis extends out to the right. The bearings shown at right angles to the gimbal axis were originally part of the dual-gimbal support for the rotor when it was used as a rate sensor. Those bearings have been staked in place so that the resulting system in a single-gimbal CMG.

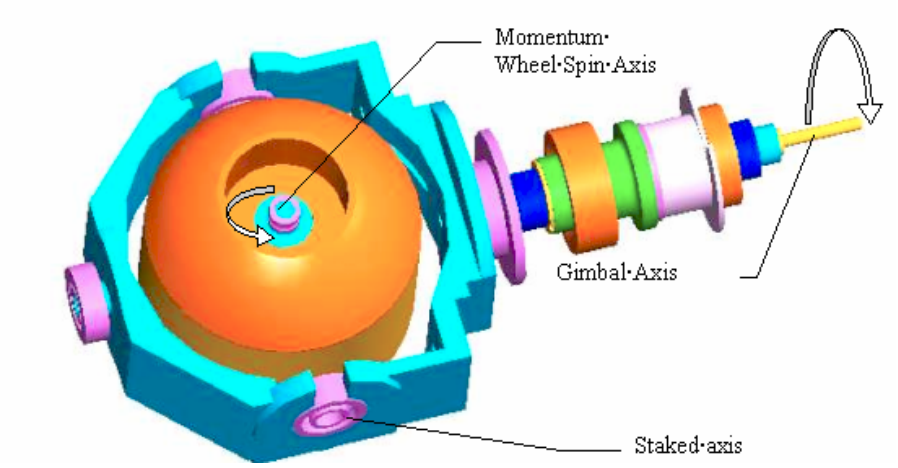

Figure 5. Inner Gimbal Configuration (Some Components not Shown, for Clarity)

Again, since the Testbed is meant for MCS research, each CMG's gimbal axis can be reoriented, via the adjustable fixture shown in Figure 6, so that the CMG array can represent virtually any geometry of interest. The MCS includes six of these tiny CMGs mounted by means of these fixtures to a common palette that the Vibration Isolation and Steering System (VISS) supports. Figure 7 show the MCS as it is currently integrated in the testbed

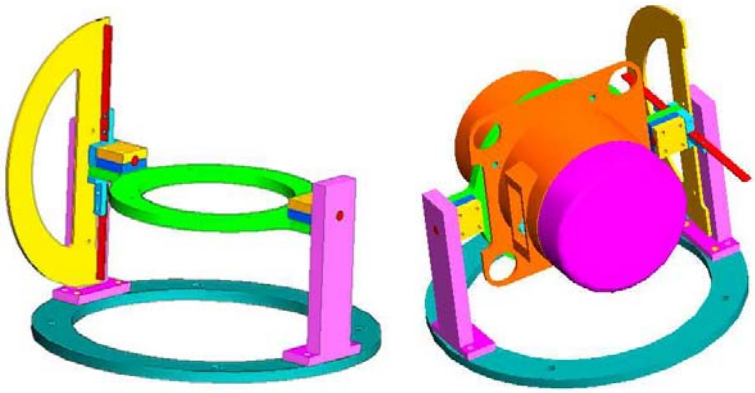

Figure 6. Adjustable Fixture for a Single CMG

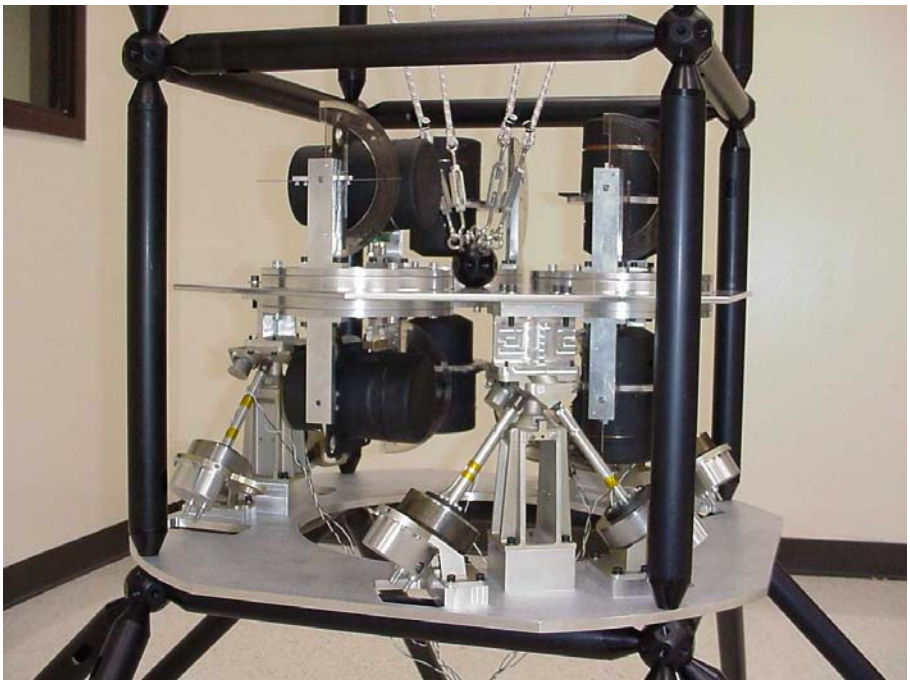

Figure 7. Six CMGs in an MCS, Including VISS

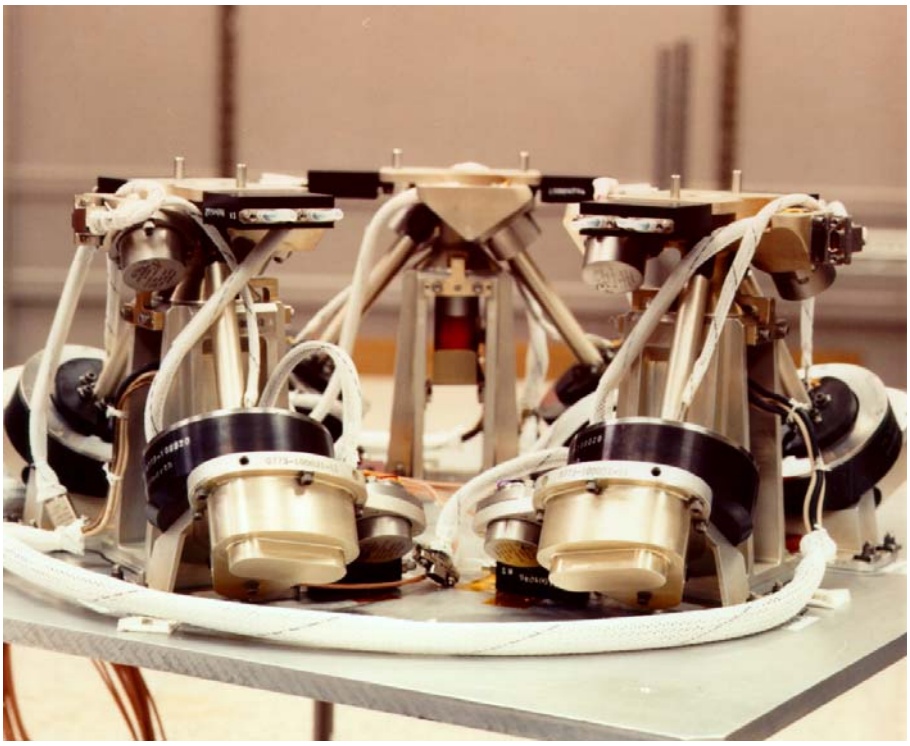

Figure 8. VISS Hexapod Assembly

The VISS system employs both passive and active structural control techniques, making it a hybrid actuator. The VISS without its MCS payload is shown in Figure 8. The passive portion of the system provides damping with break frequencies (eigenvalues) that range from 0.8 to 2.0 Hz in the six rigid body degrees of freedom. The active control improves the passive performance to achieve 20 dB of isolation at 3 Hz and above in each of the six degrees of freedom.

The passive portion of the actuator is the previously qualified and flight-proven D-Strut™. The D-Strut™ is a hermetically sealed, viscous, damping and isolation device that provides linear performance over a very large dynamic range (>105) with a threshold displacement below 1 nm. Figure 9 shows a D-Strut™ with a geometrically identical structural truss element. The static stiffness and damping values can be independently controlled. A third parameter, sometimes referred to as volumetric stiffness, can be tuned to provide controlled amplification at resonance while retaining a -40 dB/decade roll-off above resonance. The passive system further provides static support and low-frequency follow-up or tracking. This eliminates the need for active position centering and reduces power consumption relative to a purely active system. It also enables reconfiguration of the active control in the event of a single strut failure. It further provides a soft landing, as compared to a purely active system, in the event of a power interrupt or circuit failure. In such an event, a sensitive payload could otherwise be damaged even with redundancy in the active system.

Figure 9. Truss Element (Top) and Geometrically Identical Truss Element with Integral D-Strut™ (Bottom) for Use in Reconfigurable MCS Testbed Structure

The active portion of the system uses the flight-heritage voice-coil design as a prime mover and accelerometers as sensors. Although it is an integral part of the actuator, the voice coil functions in parallel with the passive damper. The action of the

voice coil enhances the low-frequency isolation and provides for vibration suppression. At higher frequencies, active control gives way to the passive system, which can provide high-frequency isolation.

Power for the MCS/LOS Testbed is provided by a fully isolated +24V system supplied by two series-connected, +12V, rechargeable, sealed lead-acid batteries. The +24 volts is then distributed throughout the MCS/LOS Testbed to various DC-DC converters and DC-AC power inverters through a power distribution module. Table 2 lists some details.

Table 2. Power Requirements for MCS/LOS Testbed Components

Testbed Component	Voltage required	Source	Switched/ Fused
Power	+24	PS-121000 batteries	
Distribution	+12	Lambda X10-24S12	F
Module			
Mass Balancer	+24	Datel BMP-12/1.65-D24	SF
	115VAC 60 Hz	Exeltech XP-125	SF
dSPACE	+5	Power-One HBS150YG-A	SF
	±12	Datel BMP-12/1.65-D24	SF
	+6.5	LM317	S
CMG support	+24	Power Dist. +24 out	SF
electronics	115VAC 400 Hz	Exeltech XP-125	SF
IMU	+5	Datel UWR-5/2000-D24E	SF
	+15	Datel UMP-15/2.5-D24	SF
	-15	Datel UWR-15/335-D24	SF

The two series-connected +12V batteries are Power Sonic PS-121000 100 Ah, rechargeable, sealed lead-acid batteries. The worst-case time estimate to discharge the batteries is less than an hour. However, under normal discharge rates, the batteries have been used for more than 10 hours before requiring recharge. The power-distribution module contains circuitry that monitors the battery voltage to prevent excessive discharge. At a bus voltage of 22V, a warning flag is sent to the dSPACE processor on a single digital I/O line module, alerting the testbed operator and starting a sequence of fault responses. At 21V the main power relay located in the power distribution module is switched to an open state, and power to testbed is disconnected. As an alternative to powering the system with batteries, a commercial AC-to-DC power supply (50 amp minimum rating) power the testbed when the battery system is disconnected. This allows operation or checkout of the system during a time when the batteries are undergoing a recharge cycle. It can also be used to run up the CMG rotors to conserve battery power.

The structure of the MCS/LOS Testbed consists primarily of truss elements manufactured by the Midé Corporation. These truss elements can be configured to represent booms, solar arrays, antennas, and other large structures of interest in flexible-dynamics analysis. At present, the testbed is built to ensure high bending stiffness to

prevent anisoelastic effects[4,5] from introducing mass-center offset that would tend to saturate the CMGs. In 2004 a more representative spacecraft bus model will replace this truss structure, as described in the section on the 2004 project.

Figure 10. MCS/LOS Testbed Configuration with Guy Wires for Bending Stiffness

Although it is somewhat disingenuous to claim that this testbed includes a propulsion system, it does include means of controlling the position of its mass center. Foremost, of course, is the spherical airbearing that supports the structure. Manufactured by Guidance Dynamics Corporation, It is mounted on a 10,000 lb concrete block which is isolated from the rest of the building in an effort to reduce the effects of seismic vibrations. It can levitate over 3000 lb. The 2003 testbed weighs only about 1200 lb, but the 2004 system will be closer to the limit. It uses less than 2 cfm at 120 psi for its maximum load. The range of motion allows $\pm$ 30^o of motion about any horizontal axis and unconstrained rotation about the vertical. In addition, the testbed includes three prismatic actuators (produced by Parker Automation) with very fine position control that are used to calibrate and balance the testbed. Although active balance is possible with these devices, they are instead used in a calibration step before maneuvering begins so that their motion does not introduce unrealistic dynamics during testing.

Any offset $\boldsymbol{c}$ of the mass center offset from the airbearing's center of rotation would tend to introduce a pendulum-like torque due to gravity $\boldsymbol{g}$:

$$\boldsymbol{\tau} = \boldsymbol{c} \times M\boldsymbol{g}\,, \tag{1}$$

where M is the mass of the testbed. For 30 minutes of maneuvering uninterrupted by CMG saturation, the mass center must be less than about 2.4 μin in the plane perpendicular to $\boldsymbol{g}$. Although reaching this goal might seem hopeless, the masses on the balancer hardware (shown in Figure 11) can be positioned to within 40 μin. The influence of a component's mass m on the system mass center goes with $m/(m+M)$, with the result that moving mass of about 40 lb or less offers enough resolution to meet the balance-calibration requirements. This fine control is the principal motivation for using closed-loop balance calibration; achieving it manually would likely consume an inordinate amount of time.

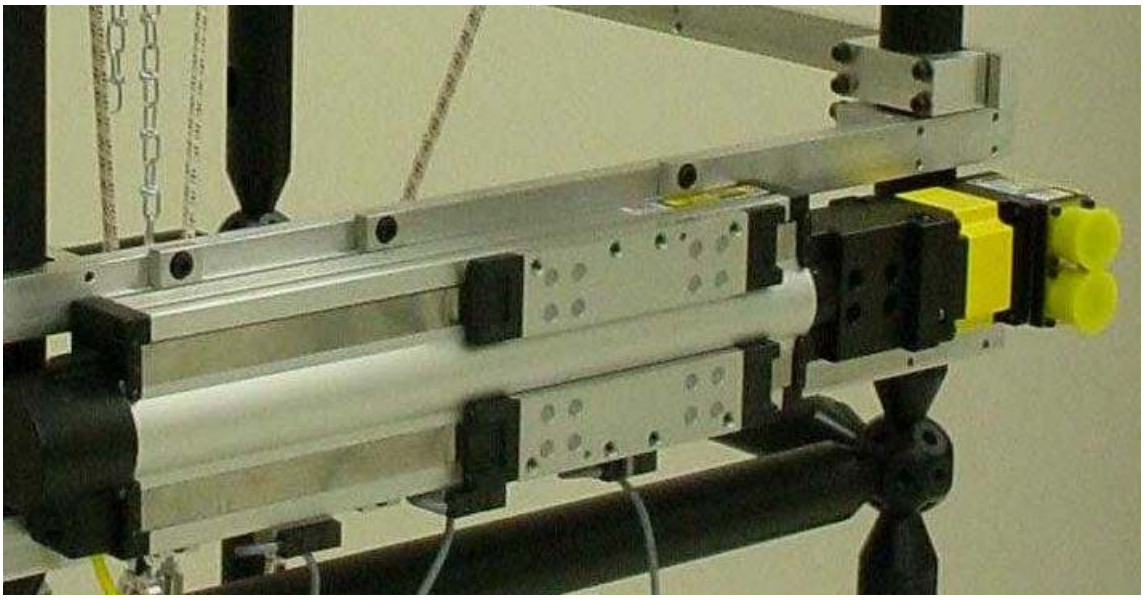

Figure 11. One of the Three Mass Balancers on the MCS/LOS Testbed, Shown without Proof Mass.

The payload of the MCS/LOS Testbed is its MCS. However, other hardware can be integrated on the testbed and its performance verified and validated in the presence of realistic, coupled attitude dynamics and structural dynamics. The pointing performance of such line-of-sight-intensive payloads is measured with the LOS Scoring system, components of which are shown in Figures 12 and 13. This system includes three CCDs

Figure 12. LOS Scoring System Consisting of Three Lasers and Three CCDs with Centroiding Software, Mounted on a Newport Pneumatically Isolated Optical Bench

Figure 13. Mirrors Mounted on the Testbed that Reflect Light from the Lasers and Back into the CCDs, Used to Estimate Angular Jitter.

and centroiding software from Duma Optronics that capture the light emitted from three lasers and reflected off three mirrors mounted on the testbed. The testbed carries three sets of three mirrors each, allowing jitter to be measured at various testbed attitudes (such as before and after a slew maneuver). The CCDs and lasers are mounted on a pneumatically isolated optical bench, where the CCDs are sampled at 30Hz. The six pieces of focal-plane data are resolved into unit vectors and from there combined to provide a least-squares estimate of the direction-cosine matrix at the location of the mirrors using Markley's SVD method[6]. Thus, three-axis jitter measurements are available at a Nyquist frequency of 15 Hz. The 2003 testbed will offer an increased data rate. Table 3 summarizes some of the performance parameters of the current LOS Scoring System. It has been shown to detect jitter below 1μrad RMS.

Table 3. Scoring-System Parameters

	Bare Detector	**Augmented with 3" Aspherical Lens**
detector width	0.0062 m	0.0762 m
laser to detector	2 m	2 m
sample frequency	30 Hz	30 Hz
desired # samples	100	100
Max. scan-maneuver rate	0.0009 rad/sec	0.0114 rad/sec
	0.0533 deg/sec	0.6549 deg/sec
Number of pixels	721	721
Effective pixel size	8.59917E-06 m	0.00011 m
Centroiding reduction	0.1	0.1
Angular resolution	4.30E-07 rad	5.28E-06 rad
	0.43 μrad	5.28 μrad
	2.46E-05 deg	3.03E-04 deg

SOFTWARE AND ALGORITHMS

While describing the MCS/LOS Testbed's command and control architecture in its entirety would require too much space, we present here some highlights of our algorithms that are arguably a new addition to the field of airbearing testbed dynamics and control. Foremost among these algorithms is a suite of approaches to center-of-mass compensation. This section summarizes four potential approaches: adaptive compensation, precalibration using closed-loop proof-mass actuation, precalibration using discrete mass-balance configurations, and open-loop system identification.

As we argued earlier, compensating for mass-center imbalance actively during slew maneuvers introduces potentially corrupting noise from the mass-sliders. Since pains have been taken to ensure that the testbed's environmental disturbances do not interfere with sensitive jitter measurements, this approach has not been baselined.

However, it is instructive to consider the relative simplicity of the approach. The adaptive algorithm is based on a simple rigid-body model of the spacecraft, characterized by an inertia dyadic $\boldsymbol{I}$, angular velocity of a body-fixed frame B relative to an inertial frame N $\boldsymbol{\omega}^{\mathrm{B/N}}$, and a drag coefficient C that is used to fit viscous aerodynamic effects. The resulting equation of motion is

$$\boldsymbol{I}\frac{{}^{\mathrm{B}}d}{dt}\boldsymbol{\omega}+\frac{{}^{\mathrm{B}}d}{dt}\boldsymbol{h}+\boldsymbol{\omega}^{\mathrm{B/N}}\times\left(\boldsymbol{I}\cdot\boldsymbol{\omega}^{\mathrm{B/N}}+\boldsymbol{h}\right)=\boldsymbol{c}\times M\boldsymbol{g}-C\left(\boldsymbol{\omega}^{\mathrm{B/N}}\cdot\boldsymbol{\omega}^{\mathrm{B/N}}\right)^{\frac{1}{2}}\boldsymbol{\omega}^{\mathrm{B/N}}, \tag{2}$$

where $\boldsymbol{h}$ represents the angular momentum in the CMGs as discussed elsewhere[7]. Projecting this equation onto a set of orthogonal body-fixed basis vectors $\boldsymbol{b}_{\mathrm{i}}$ and collecting on the 10 unknown parameters yields a linear matrix relation:

$$\left[\tilde{\dot{\omega}}+\omega^{\times}\tilde{\omega}\quad g^{\times}\quad\left(\omega^{\mathrm{T}}\omega\right)^{\frac{1}{2}}\omega\right]\begin{bmatrix}\tilde{I}\\ Mc\\ C\end{bmatrix}=\dot{h}+\omega^{\times}h, \tag{3}$$

where the $\tilde{}$ operator indicates a reordering of matrix components such that

$$I\omega=\tilde{\omega}\tilde{I}, \tag{4}$$

i.e.

$$\tilde{\omega}=\begin{bmatrix}\omega_1 & 0 & 0 & \omega_2 & \omega_3 & 0\\ 0 & \omega_2 & 0 & \omega_1 & 0 & \omega_3\\ 0 & 0 & \omega_3 & 0 & \omega_1 & \omega_2\end{bmatrix}, \tag{5}$$

and

$$\tilde{I}=\begin{bmatrix}I_{11} & I_{22} & I_{33} & I_{12} & I_{13} & I_{23}\end{bmatrix}^{\mathrm{T}}. \tag{6}$$

The notation $^{\times}$ indicates the skew-symmetric matrix equivalent of the cross-product operation, e.g.

$$g^{\times}=\begin{bmatrix}0 & -g_3 & g_2\\ g_3 & 0 & -g_1\\ -g_2 & g_1 & 0\end{bmatrix}, \tag{7}$$

With equation (3) any number of least-squares estimators for the system parameters can be developed, as described in previous work in this area[8]. The estimated

parameters can be used adaptively to trim the performance or they can be used to set the mass balancers to an optimal configuration in preparation for collecting data with the testbed. A similar result uses the known gravity-induced moments due to certain well-known mass items to enrich the data on the right-hand-side of equation (3) and improve the estimate of the parameters.

The preferred approach to mass-balance compensation is to precalibrate the mass balancers. This approach can take two forms: one in which the ACS and mass-balancer control work in concert to drive the system to a torque-free, non-spinning equilibrium and another in which mass-balancer displacements are established manually and the ACS is allowed to settle the attitude to a torque-free equilibrium. Whichever approach is taken, a collection of discrete measurements of equilibrium states is combined as follows. First, we assume that a unit vector in the direction of gravity, $\hat{g}_i$, is known in testbed coordinates for the i^{th} measurement. It can be propagated via the gyro, measured indirectly from the LOS scoring system, or measured directly from the accelerometer within the testbed's IMU. For more than two measurements, we note that all measurements in equilibrium require that the mass imbalance perpendicular to gravity be zero:

$$\left(\mathbf{1}-\hat{g}_i\hat{g}_i^{\mathrm{T}}\right)\left(MR+\sum_{j=1}^{3}m_j\left(r_j+d_{j,i}s_j\right)\right)=0\,, \tag{8}$$

where r_i is the nominal location of the j^{th} mass balancer, $d_{j,i}$ is the displacement of that balancer for the i^{th} measurement, m_i is its mass, and s_i is a unit vector along its path of travel. Stacking n measurements results in a linear matrix relation that can be solved as a batch least-squares problem for the total imbalance, and thence the optimal combination of mass-balancer displacements that balances a rigid system:

$$MR=\begin{bmatrix}\mathbf{1}-\hat{g}_1\hat{g}_1^{\mathrm{T}}\\ \mathbf{1}-\hat{g}_2\hat{g}_2^{\mathrm{T}}\\ \vdots\\ \mathbf{1}-\hat{g}_n\hat{g}_n^{\mathrm{T}}\end{bmatrix}^{+}\begin{bmatrix}-\left(\mathbf{1}-\hat{g}_1\hat{g}_1^{\mathrm{T}}\right)\left(\sum_{j=1}^{3}m_j\left(r_j+d_{j,1}s_j\right)\right)\\ -\left(\mathbf{1}-\hat{g}_2\hat{g}_2^{\mathrm{T}}\right)\left(\sum_{j=1}^{3}m_j\left(r_j+d_{j,2}s_j\right)\right)\\ \vdots\\ -\left(\mathbf{1}-\hat{g}_n\hat{g}_n^{\mathrm{T}}\right)\left(\sum_{j=1}^{3}m_j\left(r_j+d_{j,n}s_j\right)\right)\end{bmatrix}, \tag{9}$$

To find the d_j to be commanded for complete mass-center balance, we recall that when the system is balanced,

$$0 = MR + \sum_{j=1}^{3} m_j \left(r_j + d_j s_j \right). \tag{10}$$

Therefore, using a Jacobian that maps from physical coordinates into mass-balancer axes,

$$\begin{bmatrix} d_1 \\ d_2 \\ d_3 \end{bmatrix} = \begin{bmatrix} m_1 s_1 & m_2 s_2 & m_3 s_3 \end{bmatrix}^{-1} \left(-MR - \sum_{i=j}^{3} m_j r_{j,0} \right). \tag{11}$$

The product MR is merely a placeholder here; the RHS of equation (9) can be substituted instead, eliminating the step of recording the position of the testbed mass center if the objective is merely balance. There is an arbitrary scale factor here, one associated with the units of measurement for the mass-balancer positions. The position can be recorded in any convenient units, such as the step count of a stepper motor, and the result of equation (11) will be computed in those units.

2004 PROJECT

In 2004 the capabilities of the existing system will be enhanced so that it represents state-of-the-art spacecraft dynamics with an unmatched degree of fidelity. Careful planning over the past two years has ensured that much of the progress in 2002 (including hardware and software development) can be applied directly to the 2003 effort. The 2003 testbed will use six 225 ft-lb-sec CMGs with custom passive isolation to control a 1/3-scale spacecraft structure. The structure includes architectural entry points for structural control, such as D-Struts™, and offers a means for simulating payload-pointing performance. A more advanced LOS scoring system, based on interferometry, will measure this jitter performance. Also, higher-precision sensors (including Honeywell's miniature IMU[9] and an in-house developed star tracker) will offer a lower-noise environment for assessing MCS control.

Table 4 compares the 2002 system with what is planned for 2003. Figure 13 is a sketch of the 2003 system showing 6 CMGs. Not shown in the sketch are the flexible bodies that will be used to model appendage modes. These bodies are designed so that the mass center of each coincides with the point on which they are pivoted, although the inertia matrix can be arbitrary. A rotational spring and (optionally) damper provide a single appendage mode for each body, which is otherwise very stiff; thus, its motion does not introduce mass-offset that would otherwise tend to worsen anisoelasticity. This solution allows low-frequency structures to be included in a testbed while keeping the mass center close to the airbearing's center of rotation.

Table 4. 2002 System vs. 2003 System

Parameter	2002 MCS/LOS Testbed	2003 MCS/LOS Testbed
Number of CMGs	6	6
Angular Momentum per CMG	0.25 ft-lb-sec	225 ft-lb-sec
Torque per CMG	1.0 ft-lb	225 ft-lb
MCS Structural Control	Hybrid Active/Passive VISS (STRV Heritage)	Large-scale passive system
Airbearing Range	$\pm 30^o$ about any inertial horizontal axis; unconstrained about the inertial vertical axis	$\pm 30^o$ about any inertial horizontal axis; unconstrained about the inertial vertical axis
Mass	700 lb	3000 lb
Moments of Inertia (sl-ft^2)	22, 34, 30	600, 1000, 1000
Payload	Passive hard-mounted mirrors	Actively driven gimbaled device
Jitter Measurement Resolution (RMS)	<1 μrad	<10 nrad
Power	2 12 V Batteries	TBD
Structural Frequencies	>5 Hz	Local Modes 0.5-15 Hz on a stiff bus
Embedded Control	dSPACE	dSPACE
Rate Sensing	Ring-Laser Gyro (~1^o/rt-hr drift)	Micro IMU (~$.01^o$/rt-hr drift)
Attitude Sensing	LOS Scoring System Feedback	Ad-hoc Star Tracker
Structural Damping	Nothing Explicit Other than VISS	Discrete D-Struts™

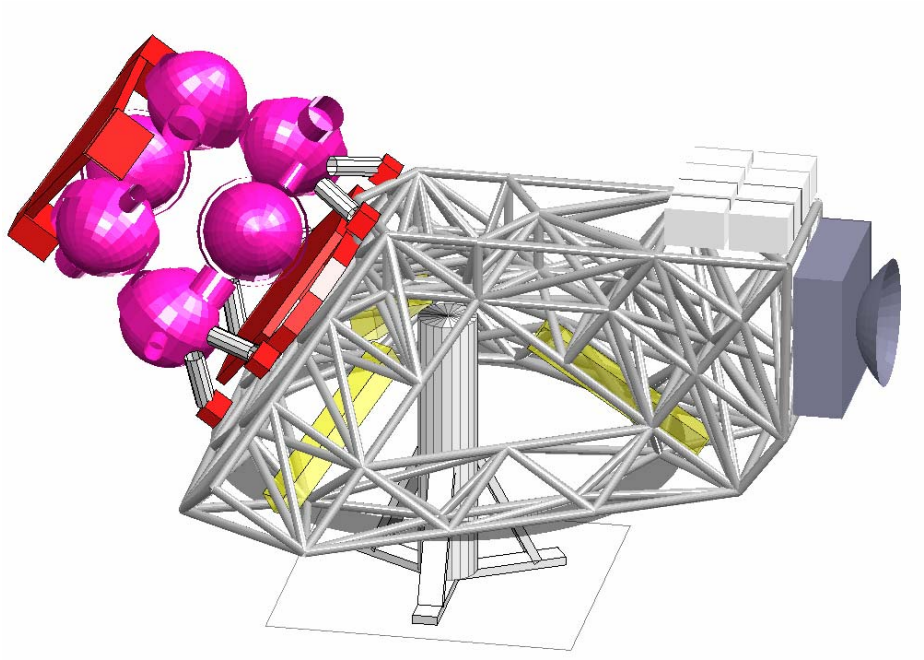

Figure 14. 2003 Testbed Structure with 6 225 ft-lb-sec CMGs

CONCLUSION

To date the MCS/LOS Testbed project has yielded results for research into the hardware performance and software architecture of an MCS in terms of its ability to reduce payload jitter and provide momentum despite internal CMG singularities. In the first half of 2004 the smaller testbed will be used to demonstrate MCS-resident fault-response capabilities and integral CMG-array singularity avoidance. The transition to the larger system is expected to occur in mid-to-late 2004, with an operational large-scale system available by the end of the year.

REFERENCES

[1] J. L. Schwartz, M. A. Peck, and C. D. Hall, "Historical Review of Spacecraft Simulators" in *Proceedings of the AAS/AIAA Spaceflight Mechanics Meeting*, no. AAS 03-125, Ponce, Puerto Rico, February 10-13, 2003.

[2] T. Hintz, T. Davis, and T. Hoffman, "IPD Design Processes Used on the STRV-2 Vibration Isolation Steering and Suppression System," AIAA Paper 96-268, 1996.

[3] P. Davis, D. Carter, J. Sullivan, T. Hoffman, and A. Das, "Vibration Isolation System Using Hybrid Dstrut™ Technology for Precision Payloads", 19th Annual AAS Guidance and Control Conference, February, 1996.

[4] G. A. Smith, "Dynamic Simulators for Test of Space Vehicle Attitude Control Systems," in Proceedings of the Conference on the Role of Simulation in Space Technology, Part C, pp. XV-1-XV-30, Blacksburg, Virginia, August 17-21, 1964.

[5] H. Mork and P. Wheeler, "Three-Axis Attitude Control System Air-Bearing Tests with Flexible Dynamics", Paper no. 73-866, in Proceedings of the AIAA Guidance and Control Conference, Key Biscayne, Florida, August 20-22, 1973.

[6] F. L. Markley "Attitude Determination Using Vector Observations and the Singular Value Decomposition," Journal of the Astronautical Sciences, Vol. 36, No. 3, July-Sept, 1988, pp. 245-258.

[7] M. Peck, "Estimation of Momentum Wheel and CMG Alignments from On-Orbit Telemetry," Proceedings of the 2001 Flight Mechanics Symposium, NASA/Goddard Space Flight Center, Greenbelt, Maryland, June 2001.

[8] M. Peck, "Estimation of Inertia Parameters for Gyrostats Subject to Gravity-Gradient Torques," Proceedings of the 2001 AAS Astrodynamics Specialist Conference, Quebec City, Canada, July 2001.

[9] B. Garavelli, L. Marradi, and A. Morgan, "Space-Qualified GPS Receiver and MIMU for an Autonomous on-Board Guidance and Navigation Package." Paper no. 2583 in SPIE Proceedings Vol. 2583, Advanced and Next-Generation Satellites, Paris, France, September 25–28, 1995, pp. 539-54.